

XANES investigation of the local structure of Co nanoclusters embedded in AgGuilin Zhang,¹ Z. Y. Wu,^{2,3} Aiguo Li,¹ Yinsong Wang,¹ Jing Zhang,² M. I. Abbas,² R. Hu,²
Xinbo Ni,¹ Yongpeng Tong,¹ and Yeukunng Hwu⁴¹Shanghai Institute of Nuclear Research, Chinese Academy of Science, Shanghai 201800, China²Beijing Synchrotron Radiation Facility, Institute of High Energy Physics, Chinese Academy of Sciences,
P.O. Box 918, 100039 Beijing, People's Republic of China³Laboratori Nazionali di Frascati, Istituto Nazionale di Fisica Nucleare, Via Enrico Fermi 40, I-00044 Frascati, Italy⁴Institute of Physics, Academia Sinica, Nankang Taipei 11529, Taiwan, Republic of China

(Received 29 September 2003; published 11 March 2004)

Ion-implanted cobalt atoms into a silver matrix with a layer thickness of about 20 nm were studied by x-ray absorption near-edge spectroscopy (XANES) at the Co *K* edge. Full multiple scattering *ab initio* calculations of Co XANES at the *K* edge provide a phase fingerprint to distinguish the Co structure of samples prepared at different doses and annealing temperatures. The bcc Co phase is formed for the as-prepared sample with 6 at. % and the fcc Co phase is formed at the expense of the bcc phase for the sample with 12 at. % after annealing at 400 °C.

DOI: 10.1103/PhysRevB.69.115405

PACS number(s): 61.46.+w, 36.40.Mr

I. INTRODUCTION

Bulk Co has a hcp crystal structure at room temperature, and transforms to fcc above 425 °C. In rare cases the uncommon bcc phase can be found.^{1,2} Other possible forms such as truncated octahedral, icosahedra or chainlike agglomerates have been reported.^{3–5} Clusters of Co embedded in Ag, however, generally show a fcc structure.⁶ Contrary to these findings, using x-ray absorption near edge structure (XANES), assisted with a full multiple scattering (MS) *ab initio* calculation of the Co *K*-edge spectra, we identified a bcc phase in samples prepared by ion implantation of cobalt atoms into a silver matrix with a layer thickness of about 20 nm.

Effects such as the giant magnetoresistance in Co/Cu and Co/Ag films^{7,8} and the increase of the magnetic moment per atom⁹ are known to depend dramatically on the shape, the size, and the phase of the clusters. Therefore the precise confinement of the nanoclusters in a matrix and their evolution under a thermal treatment are crucial to the overall properties of the granular films. However, the determination of the structure of Co clusters formed by ion implantation is generally hindered by the small quantity of Co atoms contained in the matrix and by other special reasons such as the nearly identical hyperfine fields of Co in the hexagonal and the cubic forms.^{10,11} It is, for instance, not a trivial task to determine the phase by Mössbauer spectroscopy and /or by NMR for nonhomogeneous Co clusters. Since the coordination numbers of the first and second shells of Co hcp and fcc structures are quite similar, and since ion implantation of Co in Ag produces very small clusters embedded in a shallow region, the application of an extended x-ray absorption fine structure analysis is also very cumbersome. Therefore, we need a more accurate method to distinguish the different possible phases. In this work we demonstrate that useful structural information on such nanoclusters can be extracted by XANES.¹² Lacking reference spectra from rare atomic arrangements such as the bcc phase of Co, we used instead a full MS *ab initio* calculation to generate them. We found that the difference between different structures is sensitively reproduced and that the theoretical calculation matches the ex-

perimental data in an excellent way, enabling us to identify the phases and their evolution.

The embedded Co clusters were formed by ion implantation. Silver was chosen as a host matrix since Co is immiscible with Ag and tends to occupy substitutional sites or aggregate in the host Ag matrix lattice. The thermal annealing procedure was used to study the Co cluster phase transition.

II. EXPERIMENT

Four silver polycrystalline foils were used as substrates, with a thickness of 60 μm and a purity of 99.99%. Before ion implantation the samples were annealed in a hydrogen atmosphere at 800 °C. The Co ions were implanted in the substrate at room temperature (20 °C) by the mass separator in the Shanghai Institute of Nuclear Research. The energy for the Co ions was 70 keV, corresponding to a mean range of 20 nm calculated by TRIM (transport and range of ions through matter). The doses of 1.5×10^{16} and 3×10^{16} atoms cm⁻² were chosen for two pairs of samples. Their corresponding concentrations in Ag are about 6% and 12%. Two samples with two different doses were annealed in a hydrogen atmosphere at a pressure of 4×10^4 Pa at 400 °C.

XANES spectra at the Co *K* edge were measured in the fluorescence mode by using synchrotron radiation with a Si(111) double crystal monochromator at the beam line 4W1B of the Beijing Synchrotron Radiation Facility (BSRF). The storage ring worked at a typical energy of 2.2 GeV with an electron current of about 100 mA. To suppress the unwanted higher harmonics, a detuning of 30% was performed between the two silicon crystals. The incident and output beam intensities were monitored and recorded using ionization chambers filled by argon gas and a 25% argon-doped nitrogen mixture. The spectra were scanned in the range of 7.5–7.9 keV with steps of 0.5 eV and an energy resolution of 1.5 eV. Common background subtraction was employed in the data reduction and the data were normalized and calibrated to the edge of Co metal foil.

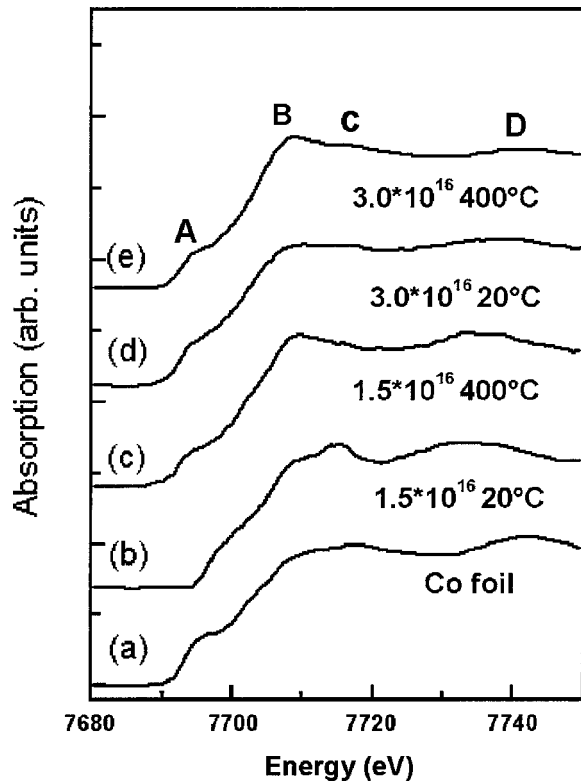


FIG. 1. XANES spectra at the Co K edge for the metallic Co foil (a), as-implanted and annealed CoAg samples [(b)-(e)], the dose (at/cm^2) and annealing temperature ($^\circ\text{C}$) are indicated in each curve.

III. CALCULATION DETAILS

Co K edge XANES spectra have been simulated via the full MS theory.¹³ In dealing with the x-ray absorption process one is faced with two fundamental problems, namely, (a) a reduction of the inherent many-body problem to the simpler scenario of one electron moving in an effective optical potential, and (b) a full description of all orders of the MS events that the excited photoelectron undergoes in its way in the system, since the perturbation expansion of the MS problem might not converge. A possible solution to these problems has been described,¹⁴ both with respect to the choice of the optical potential and to the treatment of MS to all orders of the perturbation theory (full MS). Actually, the striking success of the MS approach in dealing with the amplitude and phase problem of the fine structure oscillations in the absorption spectra¹⁵ makes one confident that this approach may also be extended to more complicated materials.¹⁶

The construction of the charge density and potential follow the same patterns as Ref. 13. We use the Mattheiss prescription¹⁷ to construct the cluster density. The Coulomb part of the potential is obtained by a superposition of neutral atomic charge densities taken from the Clementi-Roetti tables.¹⁸ For the exchange-correlation part of the potential we have used the optical Hedin-Lundqvist potential.¹⁹ In order to simulate the charge relaxation around the core hole in the photoabsorber of atomic number Z ($\text{Co}=27$) we select the $Z+1$ approximation (final state rule),^{13,19} which consists

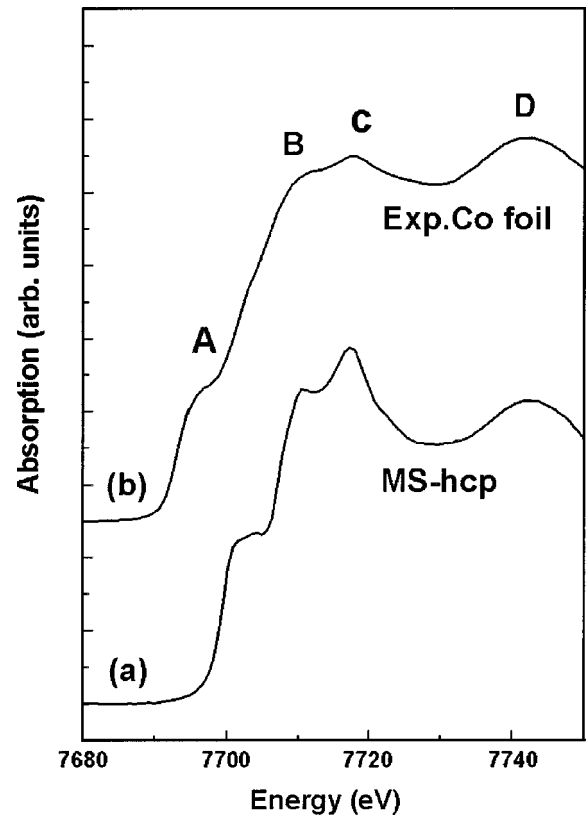


FIG. 2. XANES spectrum at the Co K edge for the metallic Co foil (b) and a simulated spectrum by the full MS theory (a).

of taking the orbitals of the $Z+1$ atom and constructing the charge density by using the excited electronic configuration of the photoabsorber with the core electron promoted to a valence orbital. The calculated spectra are further convoluted with a Lorentzian shaped function with a full width 2.8 eV (Ref. 20) to account for the core hole lifetime and the experimental resolution. We have chosen the muffin-tin radii according to the Norman criterion,²¹ and allowed a 7% overlap between contiguous spheres to simulate the atomic bond.²²

IV. RESULTS AND DISCUSSION

The near-edge fine structures of the K -edge absorption spectra are the fingerprints of the local geometry around the absorbing atom, since it is driven by multiple correlation functions beyond the mere pair one. Figure 1 presents the Co K -edge XANES spectra, arranged from top to bottom as a function of different preparation and condition (i.e., dose and annealing temperature). Also shown in Fig. 1 is the Co K -edge spectrum of pure hcp Co metal, which is in good agreement with other published work.² For convenience, all spectra are scaled so that the intensity of the main feature is the same in each spectrum. All these spectra display four main features denoted by A, B, C, and D in order of increasing photon energy. Several variations in these spectra are monitored, such as the relative intensity of peaks B and C and the separation between peaks B and D. All these changes in the spectra could be interpreted in terms of the first-shell and the next-nearest local structure around the photoab-

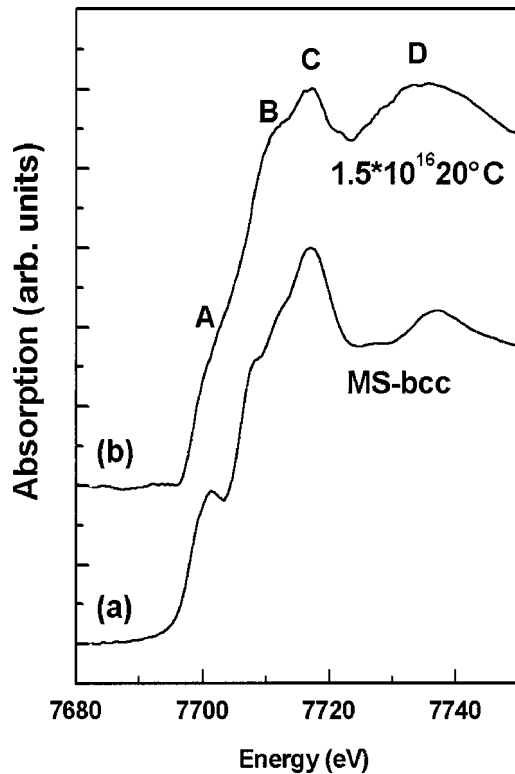


FIG. 3. XANES spectrum at the Co K edge for the as-implanted sample with a dose of 1.5×10^{16} at/cm² (b) and a simulated spectrum by the full MS theory (a).

sorber, due to the different multiple scattering processes.

The experimental Co K -edge XANES spectrum of pure hcp Co foil is compared in Fig. 2 with the *ab initio* calculated XANES using full MS theory with a relaxed final-state potential for a finite large cluster which contains 195 atoms within a radius of 8 Å from the central Co atom. The hexagonally close-packed Co atom, surrounded by two nearest neighbors (6 + 6) at 2.497 and 2.507 Å, respectively, shows two transition peaks with an energy separation of about 31 eV between peaks B and D. The agreement between the theory using the pure Co hcp crystalline data and experimental data is quite good. Features A, B, C, and D can also be assigned unambiguously to one-electron excitations. These states are due to multiple-scattering resonances of the p photoelectron in the continuum, i.e., the maxima of the local density of states at the Co site of p type selected by the dipole selection rule ($\Delta l = \pm 1$).

In Fig. 3 we present the experimental data of the sample as implanted with 1.5×10^{16} atoms cm⁻², along with the MS calculation using a bcc cluster containing 181 atoms within a 8-Å sphere. In this structural phase, the central atom is surrounded by two subshells, eight atoms at 2.46 Å and six at 2.84 Å respectively. The spectrum is very clearly different from that of the standard Co hcp foil as shown in Fig. 1 [curve (a)] and/or in Fig. 2. We found a different energy separation between peaks B and D which is now about 8 eV smaller than in Fig. 2. However, a very good agreement between the experimental and theoretical spectra has been

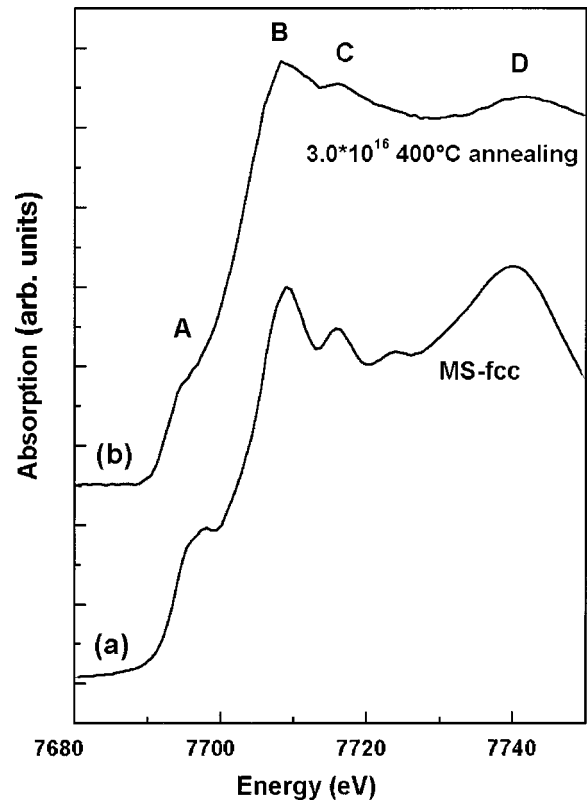


FIG. 4. XANES spectrum at the Co K edge for the sample with a dose of 3.0×10^{16} at/cm² after annealing at 400 °C (b) and a simulated spectrum by the full MS theory (a).

achieved, demonstrating that the phase transformed from a hcp to a bcc structure.

In Fig. 4 we show the experimental XANES data of the sample implanted with 3.0×10^{16} atoms cm⁻² after annealing at 400 °C. It was found that the spectral behavior significantly deviated from the previous two (typical hcp and bcc fingerprints), not only for the relative intensity of peaks B and C but also for the energy separation of the B and D features (about 33 eV). A theoretical MS calculation using a Co fcc crystalline structure (12 nearest neighbors at 2.50 Å) with a 201-atom cluster resembles the experimental data, indicating that in this case a transformation from an hcp to a fcc-like phase takes place.

The samples prepared in the intermediate conditions, as shown in Fig. 1 [curves (c) and (d)], presumably contain two or three different phase structures. It is known that the phase as well as its size²³ of particles embedded in a matrix normally depend on the annealing temperature and on the implanted dose. Therefore, for the samples prepared under intermediate conditions the phase transformation probably did not take place completely. In those samples it is possible to form a mixed phase of bcc and fcc.

For the annealed samples the fcc and hcp Co phase structures were also found by other researchers,²⁴ but with different preparation conditions, such as sputtering. Comparing with those studies, in the implanted samples a lot of vacancies could be produced, leading to a migration enhancement of Co atoms in Ag. Consequently the grain growth in those

samples would be faster than in the ones prepared by other methods.

For the as-prepared samples, the phase structure of the grains formed at an early stage is very difficult to be determined by TEM due to its small size, being less than 2 nm for 6% Co in Ag.²⁵ Therefore no satisfactory report about that has appeared so far. It was, however, found that a bcc Co phase was stabilized in rf-sputtered Co/Fe multilayers² for a Co layer thickness lower than 2 nm and a bcc-like crystalline structure with a distorted surface was formed in a polymer matrix.²⁶ Combining those results with ours, we might suggest that crystalline Co in small size could be stabilized in a bcc phase structure. For the as-implanted Co in Ag, the Co grains might be subjected to strong stresses, leading to the formation of a metastable bcc phase. To our knowledge, this is the first time the bcc Co phase structure was observed in the as-implanted CoAg sample. This experimental result was repeated three times.

V. CONCLUSION

The bcc Co phase was formed in the as-implanted Ag foil with 6-at. % Co and the fcc phase was formed at the expense of the bcc phase in the sample with 12 at. % after annealing at 400 °C, based on the comparison between the experimental results and a theoretical simulation.

ACKNOWLEDGMENTS

G.L.Zh. acknowledges the financial support from the National Natural Science Foundation of China (10075074). Z.Y.W. acknowledges the financial support of the *100-Talent Research Program* of the Chinese Academy of Sciences and of the *Outstanding Youth Fund* (10125523) of the National Natural Science Foundation of China. The authors would like to thank A. Marcelli and H. Pattyn for valuable discussion and the staffs of BSRF for their experimental assistance.

-
- ¹G. A. Prinz, Phys. Rev. Lett. **54**, 1051 (1985).
²S. Pizzini, A. Fontaine, E. Dartyge, C. Giorgetti, F. Baudelet, J. P. Kappler, P. Boher, and F. Giron, Phys. Rev. B **50**, 3779 (1994).
³B. C. Guo, K. P. Kerns, and A. W. Castleman, Jr., J. Chem. Phys. **96**, 817 (1992).
⁴Zhi-qiang Li and Bing-lin Gu, Phys. Rev. B **47**, 13 611 (1993).
⁵G. A. Niklasson, A. Torebring, C. Larsson, C. G. Granqvist, and T. Farestan, Phys. Rev. Lett. **60**, 1735 (1988).
⁶V. Dupuis, J. Tuillon, B. Prevel, A. Perez, P. Melinon, G. Guiraud, F. Parent, L. B. Steren, R. Morel, A. Bartholemy, A. Fert, S. Mangin, L. Thomas, W. Wernsdorfer, and B. Barbara, J. Magn. Magn. Mater. **165**, 42 (1997).
⁷A. E. Berkowitz, J. R. Mitchell, M. J. Carey, A. P. Joung, D. Rao, A. Starr, S. Zhang, F. E. Spada, F. J. Parker, A. Hutten, and G. Thomas, J. Appl. Phys. **73**, 5320 (1993).
⁸J. Veres, M. Cai, R. W. Cochran, and S. Roorda, J. Appl. Phys. **87**, 8504 (2000).
⁹Feng Liu, M. R. Press, S. N. Khanna, and P. Jena, Phys. Rev. B **39**, 6914 (1989).
¹⁰G. J. Perlow, C. E. Johnson, and W. Marshall, Phys. Rev. **140**, A875 (1965).
¹¹J. Verheyden, S. Bukshpan, J. Dekoster, A. Vantomme, W. Deweerd, K. Milants, T. Barancira, G. L. Zhang, and H. Pattyn, Electron. Lett. **37**, 25 (1997).
¹²Giuseppe Faraci, Agata R. Pennisi, Antonella Balerna, Hugo Pattyn, Gerhard Koops, and Guilin Zhang, the International workshop "The Physics of Low Dimensions," Oaxaca, Mexico, January 16–20, 2000.
¹³Z. Y. Wu, S. Goda, F. Jollot, M. Gautier-Soyer, and C. R. Natoli, Phys. Rev. B **55**, 2570 (1997).
¹⁴T. A. Tyson, K. O. Hodgson, C. R. Natoli, and M. Benfatto, Phys. Rev. B **46**, 5997 (1992).
¹⁵J. J. Rehr, R. C. Albers, and S. I. Zabinsky, Phys. Rev. Lett. **23**, 3397 (1992).
¹⁶Z. Y. Wu, M. Benfatto, and C. R. Natoli, Phys. Rev. B **57**, 10 336 (1998).
¹⁷L. Mattheiss, Phys. Rev. A **134**, 970 (1964).
¹⁸E. Clementi and C. Roetti, At. Data **14**, 177 (1974).
¹⁹P. A. Lee and G. Benni, Phys. Rev. B **15**, 2862 (1977).
²⁰J. C. Fuggle and J. E. Inglesfield, *Unoccupied Electronic States, Topics in Applied Physics* (Springer, Berlin, 1992), Appendix B, p. 347.
²¹J. G. Norman, Mol. Phys. **81**, 1191 (1974).
²²Y. Joly, Phys. Rev. B **63**, 125120 (2001).
²³G. L. Zhang, L. Liu, W. Hu, W. Zhou, and J. Wang, Phys. Lett. A **119**, 251 (1986).
²⁴J. R. Regnard, J. Juanhuix, C. Brizard, B. Dieny, B. Mevel, J. Mimault, and O. Proux, Solid State Commun. **97**, 419 (1996).
²⁵Mare Hou, Mahjoub El Azzaoui, Hugo Pattyn, Joris Verheyden, Gerhard Koops, and Guilin Zhang, Phys. Rev. B **62**, 5117 (2000).
²⁶M. Respaud, J. M. Broto, H. Rakoto, A. R. Fert, L. Thomas, B. Barbara, M. Verelst, E. Snoeck, P. Lecante, A. Mosset, J. Osuna, T. Ould Ely, C. Amiens, and B. Chaudret, Phys. Rev. B **57**, 2925 (1998).